Spindle speed effect on the ISF processing of materials with different thermal conductivities

QIN Zhenyuan[1,a], GATEA Shakir[1,2,b], and OU Hengan[1,c*]

[1]Department of Mechanical, Materials and Manufacturing Engineering, Faculty of Engineering, The University of Nottingham, Nottingham NG7 2RD, UK

[2]Department of Materials Engineering, Faculty of Engineering, University of Kufa, Al-Najaf, Iraq

[a]eaxzq1@nottingham.ac.uk, [b]ezzsmg@exmail.nottingham.ac.uk, [c]h.ou@nottingham.ac.uk

Keywords: Incremental Sheet Forming, Thermal Conductivity, Springback, Surface Finish, Finite Element Method

Abstract. Incremental sheet forming (ISF) is an advanced forming technology with high flexibility and excellent adaptability. However, conventional ISF encounters challenges in processing of hard-to-deformed materials at room temperature. To address this problem, friction stir incremental forming (FSIF) has been introduced to improve material formability at high temperatures. The aim of this work is to investigate the spindle speed effect on the forming quality for materials with different thermal conductivities by using an experimental and FE simulation. The experimental results presented the combined effect of spindle speed and conductivity on the springback and surface finish of AA1050 and CP Ti Grade 1. A good agreement was obtained in the temperature increase and distribution from experimental testing and FE simulation.

Introduction

Incremental sheet forming (ISF), also known as single point incremental forming (SPIF), is characterised as a flexible sheet forming technology due to the fact that it does not require specific dies and is capable of producing components with complex shapes [1,2]. Although conventional ISF possesses some advantages as compared to other sheet metal forming processes, it is still a technical challenge to use ISF to form hard-to-deform materials. To overcome this limitation, friction stir incremental forming (FSIF) has been developed to improve the formability of the hard-to-deform materials through friction heat induced by the rotating tool [3].

Due to its high applicability and simplicity, FSIF has attracted considerable research attention in the past decade. Wang et al. [4] demonstrated the formability of AA5052-H32 and AA2024-T can be significantly improved accompanied with reasonable surface quality when applying a suitable range of rotation speed. A work by Grün et al. [5] highlighted the influence of rotation speed on the forming limit of Ti6Al4V alloy. Formisano et al. [6] revealed the effect of processing parameters on the forming temperature in FSIF by conducting experiments on the polycarbonate (PC) sheets.

Besides the above experimental observations, some numerical studies on FSIF have been also reported by researchers. In the numerical work of Li and Wang [7], the non-rotating tool with equivalent temperature was adopted to enable that the same temperature variation trend as the actual testing case with rotating tool can be achieved in highly reduced simulation time. Cai et al. [8] performed FE simulations to explore the effects of process variables, i.e., feed rate, spindle speed, wall angle and vertical step size, on temperature evolution, thickness distribution, and central bulge. The simulation results were in good agreement with the experimental results. Nguyen et al. [9] used commercial FE software Abaqus incorporating VUMAT subroutine code to evaluate the fracture behaviour of AZ31 magnesium alloy in FSIF. It was shown that the fracture depth under specific forming condition was successfully predicted by the proposed numerical model.

Although aforementioned literature provides a profound understanding about FSIF in different aspects, no attempts have been made to evaluate the combined effect of spindle speed and thermal conductivities on the quality of FSIF processed parts. Therefore, this work aims to investigate the thermal response in FSIF processing of sheet materials with different thermal properties and to provide an insight into the interrelationship between the forming quality and thermal properties of the formed parts based on experimental testing and FE simulation.

Experimental testing

In this work, the AA1050 aluminium alloy and CP Ti Grade 1 pure titanium were used as workpiece, with the dimension of 150×150×0.7mm and 150×150×0.5mm, respectively. Both materials were formed by using a high-speed steel tool with a diameter of 10mm. The physical and thermal properties of workpiece and forming tool are presented in Table1.

Table 1. The physical and thermal properties of workpiece and forming tool.

Material	Density [kg/m^3]	Poisson's ratio	Young's modulus [GPa]	Yield stress [MPa]	Specific heat[J/(kg.K)]	Conductivity [W/(m.K)]
AA1050	2700	0.33	71	90	900	231
CP Ti Grade 1	4540	0.34	105	221	520	16.4
High-speed steel	7600	0.27	200	1000	460	41

The ISF was carried out on a CNC milling machine, a hyperbolic truncated cone with continuously varying wall angles from 30° to 90° was formed by using a hemispherical tool with a diameter of 10mm. Two spindle speeds (0 rpm, 2500 rpm) were used in the test, while other process parameters remained unchanged: with feed rate of 1500 mm/min, step size of 0.5 mm, and with use of Rando HD68 lubricant. The forming forces were measured by a load cell mounted below the fixture. The temperature variation of specific tracking positions with equal spacing of 6mm (see Fig. 1) was monitored by a series of thermocouples.

Materials Research Proceedings 41 (2024) 1606-1614 https://doi.org/10.21741/9781644903131-178

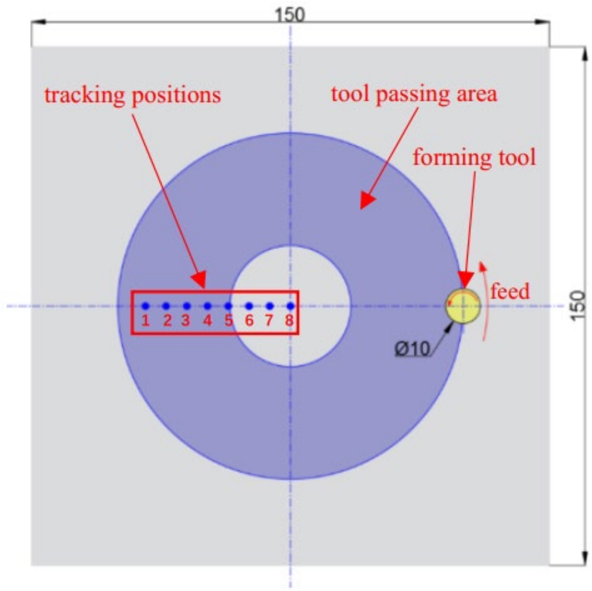

Fig. 1. FSIF tool rotation, movement and thermocouple tracking positions (unit: mm).

Finite element simulation

A coupled thermo-mechanical FE model was built in Abaqus/explicit to simulate the ISF process under specific processing condition. To obtain accurate solution to three- dimensional heat transfer problem, both workpiece and forming tool were applied with the 3D thermally coupled solid brick elements with eight nodes (C3D8T). In FE model, the workpiece was simulated as a deformable body, while the forming tool was supposed as a rigid body and its movements (along X, Y and Z directions) were constrained at a reference point. In addition, the material properties shown in Table 1 were used in FE as input values. The contact behavior at tool-workpiece interface was defined by using embedded penalty contact algorithm. By referring to previous research work, the friction coefficients were set to 0.09 and 0.167 for AA1050 and CP Ti Grade 1, respectively. The heat transfer coefficient was set to 20 W/ (m^2.K). The simulation results including forming depth and forming temperature were visualized and analysed in the output module.

Results and discussion

The forming force and forming temperature

Fig. 2 presents the variation of three components of forming forces including vertical force (F_z) and horizontal force (F_x and F_y) at different spindle speeds. For AA1050 and CP Ti Grade 1, F_z increased gradually until the peak force reached, and then monotonically decreased but exhibited different rate of decline. This can be ascribed to different flow and thinning behaviour of both materials. The variation of F_x and F_y followed a sinusoidal trend with increasing amplitude. When the workpiece was formed contour by contour, F_x and F_y shown similar patterns but with a phase difference of $\pi/2$. With increase of spindle speed, the vertical and horizontal forces displayed a drop for both materials. This is because the spindle speed has significant contribution to the friction heat, resulting in material softening effect and reduction of yield stress.

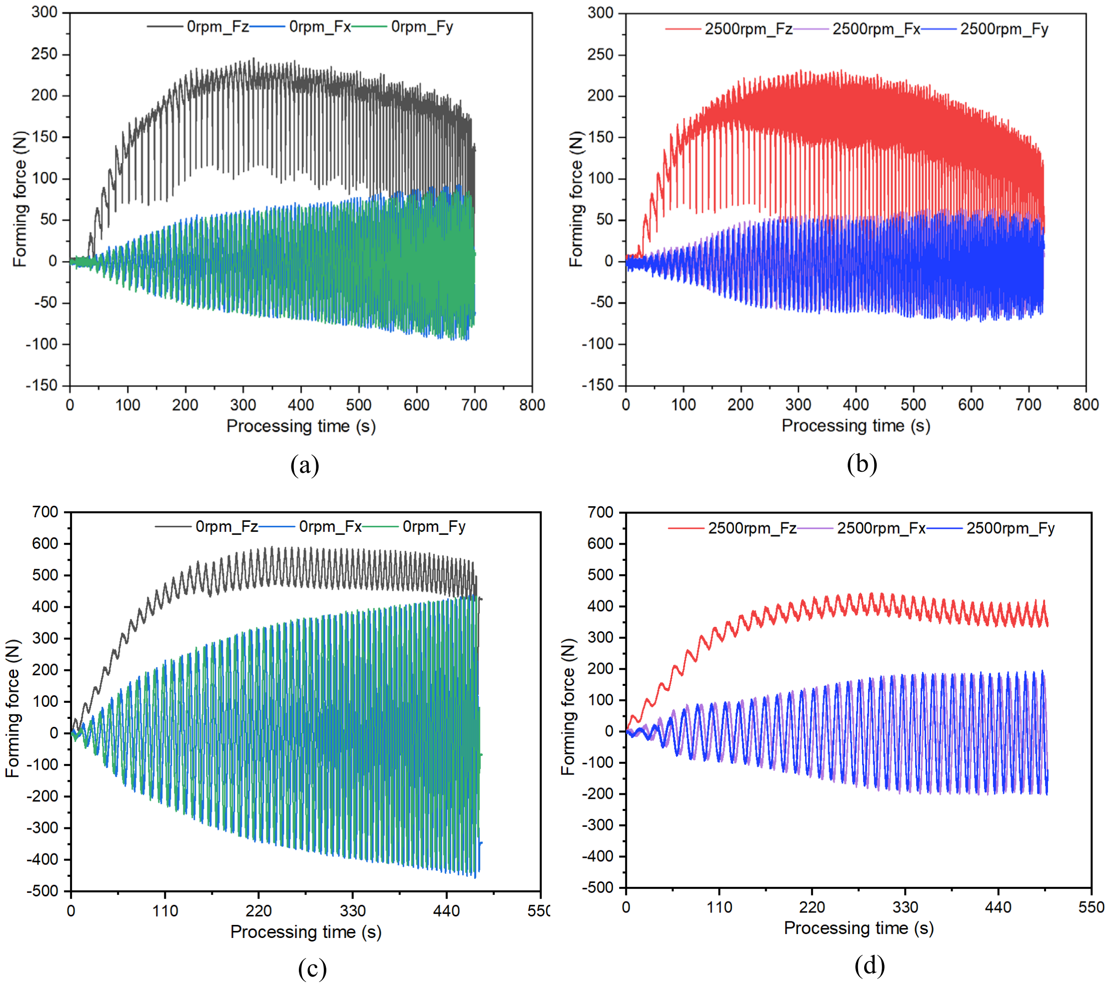

Fig. 2. The variation of forming forces for (a) AA1050 at 0 rpm (b) AA1050 at 2500 rpm (c) CP Ti Grade 1 at 0 rpm and (d) CP Ti Grade 1 at 2500 rpm.

During the testing, the temperature variation of specific tracking positions was measured by thermocouples. If these measured results are agreed with the temperature values given by FE model, the maximum forming temperature can be obtained from simulation results. The peak temperatures were measured at P4 and P3 (tracking positions shown in Fig. 1) for AA1050 and CP Ti Grade 1, respectively, after P4 and P3, the forming temperatures of the two materials reached the steady state. As can be seen in Fig. 3, as rotation speed increased from 0 rpm to 2500 rpm, the maximum forming temperature elevated from 24.6 °C to 97.45 °C for AA1050, and from 36.2 °C to 247.2 °C for CP Ti Grade 1, respectively. This dissimilar thermal response can be mainly attributed to two reasons: (i) The maximum forming force of CP Ti Grade 1 is greater than that of AA1050, leading to larger amount of friction induced heat generation. (ii) Since the thermal diffusivity and conductivity of CP Ti Grade 1 is much lower than that of AA1050, the heat flux tends to be slowly transferred from local forming zone to the surrounding regions, thereby causing obvious thermal concentration and higher temperature rise around tool-workpiece contact area. Giuseppina et al. [10] also reported similar observation and captured the effect of thermal properties on the forming temperature by performing ISF testing on AA5754 and Ti6Al4V.

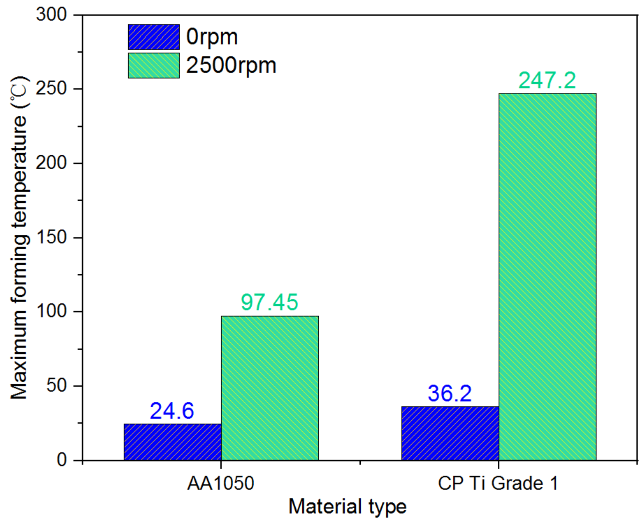

Fig. 3. The maximum forming temperature of AA1050 and CP Ti Grade 1 at different spindle speeds.

Combined effect of spindle speed and conductivity on the springback and surface finish

As discussed in above section, although under the same forming condition, a distinct difference of temperature variation was noted during processing of AA1050 and CP Ti Grade 1. This is because two determining factors (spindle speed and conductivity) are involved concurrently. Moreover, considering that the thermal effect has significant influence on the forming quality, it is necessary to study the combined effect of spindle speed and conductivity on the springback and surface finish.

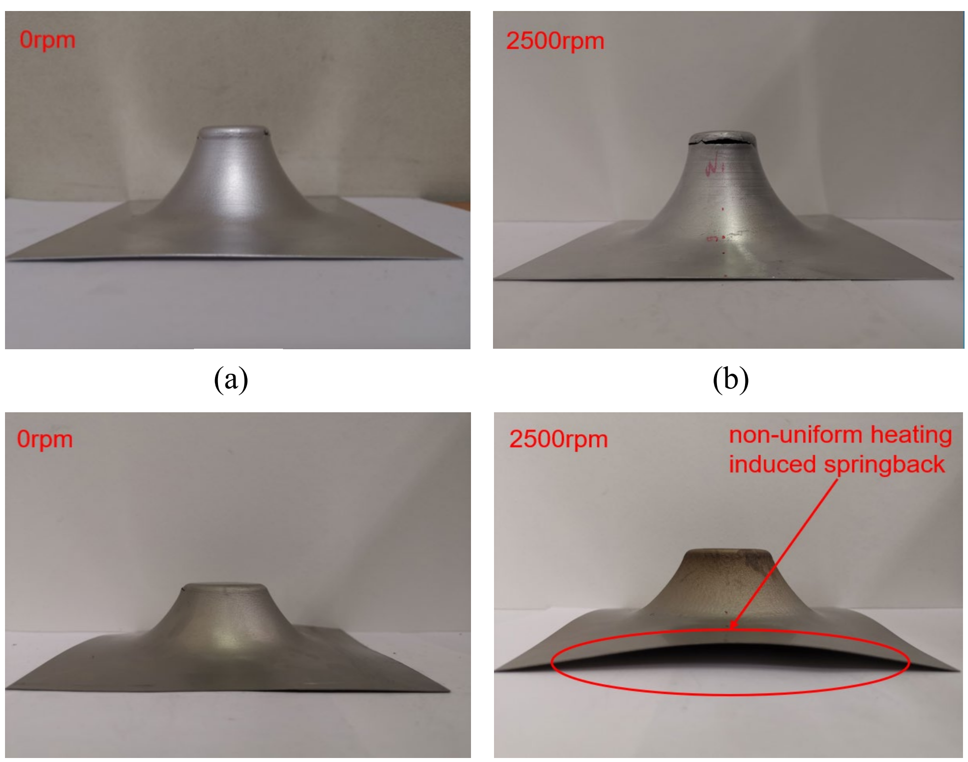

(a) (b) (c) (d)

Fig. 4. The geometry of formed part for (a) AA1050 at 0 rpm (b) AA1050 at 2500 rpm (c) CP Ti Grade 1 at 0 rpm and (d) CP Ti Grade 1 at 2500 rpm.

Fig. 4 shows the geometry of formed part for AA1050 and CP Ti Grade 1 under different processing conditions. It was noted that there was almost no springback for AA1050 at either 0 rpm or 2500 rpm, while the geometry accuracy was reasonable at 0 rpm but obvious springback occurred at 2500 rpm for CP Ti Grade 1. This is due to the fact that the thermal concentration creates high temperature difference between tool-workpiece contact area and other regions, leading to non-uniform heating induced springback for CP Ti Grade 1 at 2500 rpm. This phenomenon was also observed by Li et al. [11] through springback analysis on titanium tube. In contrast, high conductivity makes the heat flux more uniformly diffused throughout AA1050 workpiece to enable that the good geometry accuracy can be achieved at 2500 rpm.

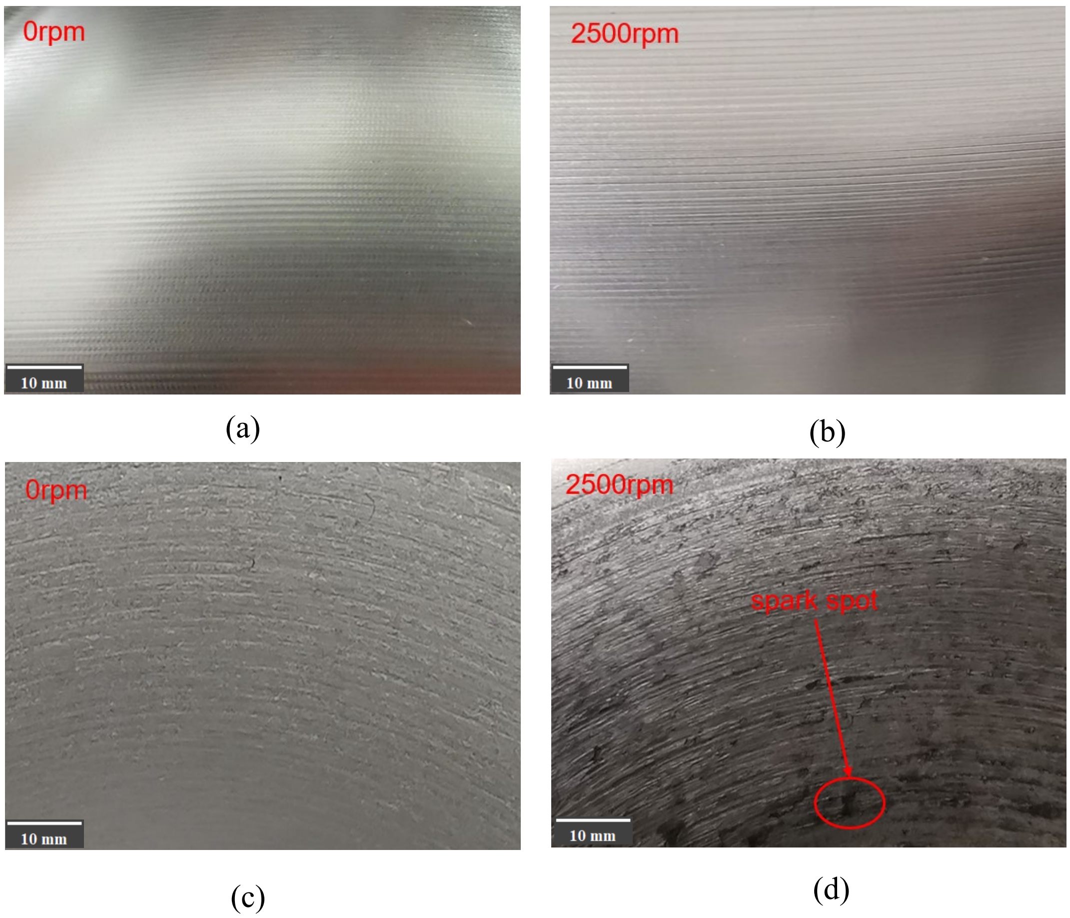

Fig. 5. The surface finish of formed part for (a) AA1050 at 0 rpm (b) AA1050 at 2500 rpm (c) CP Ti Grade 1 at 0 rpm and (d) CP Ti Grade 1 at 2500 rpm.

As can be seen from Fig. 5, under the spindle speed of 0 rpm, both AA1050 and CP Ti Grade 1 achieved acceptable surface finish; at 2500 rpm, AA1050 still had good surface finish while clear surface degradation happened for CP Ti Grade 1. This can be explained by the following reasons: firstly, the maximum shear stress of CP Ti Grade 1 is much larger than that of AA1050, which poses a negative effect on the surface quality especially at high spindle speeds. Secondly, the thermal concentration can not only locally soften the material at tool-workpiece interface, but also introduce instantaneous spark (shown in Fig. 5(d)) during the process, thereby significantly accelerating the surface degradation.

To explain the above experimental observations from a numerical perspective, FE thermo-mechanical simulations were conducted in this work. The FE models with spindle speed of 2500 rpm for both materials are shown in Fig. 6.

Materials Research Proceedings 41 (2024) 1606-1614 https://doi.org/10.21741/9781644903131-178

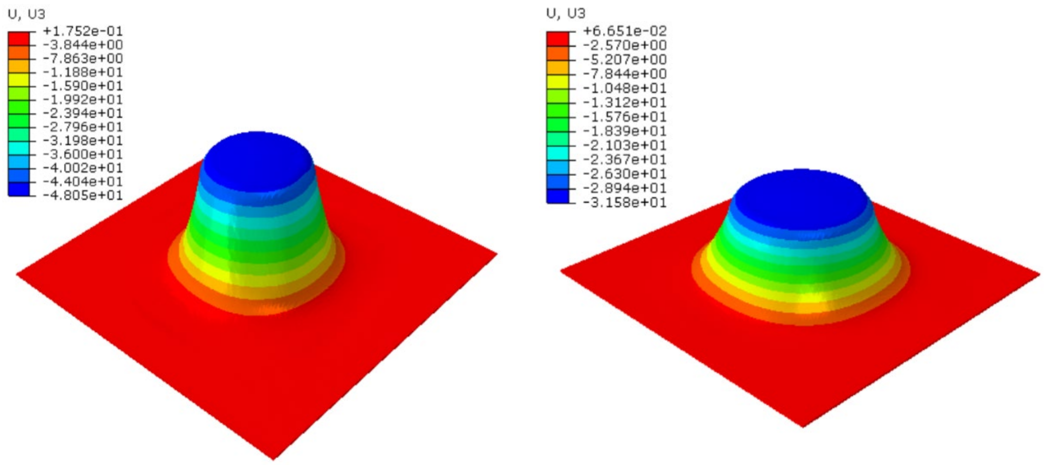

(a) (b)

Fig. 6. The FE models with spindle speed of 2500 rpm for (a) AA1050 and (b) CP Ti Grade 1.

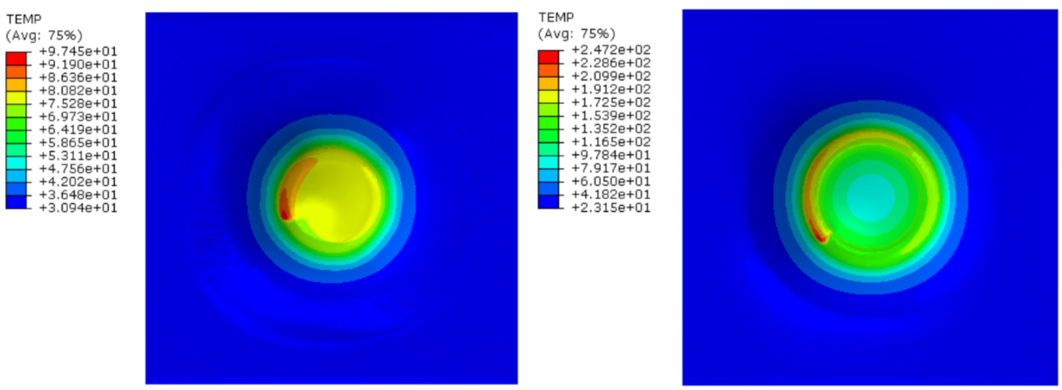

(a) (b)

Fig. 7. The temperature distribution in the final stage of process with spindle speed of 2500 rpm for (a) AA1050 and (b) CP Ti Grade 1.

Fig. 7 presents the temperature distribution in the final stage of process with spindle speed of 2500 rpm for both materials. It is evident that the temperature is distributed in an arc shape along the toolpath. The forming temperature reached the peak value at centre of tool-workpiece interface and exhibited a regular gradient from interface to surrounding regions. The maximum temperatures obtained from FE simulation were 97.45 °C and 247.2 °C for AA1050 and CP Ti Grade 1, respectively, which were slightly larger than the measured by thermocouples (95.1 °C for AA1050 and 239.7 °C for CP Ti Grade 1). Although the maximum temperature of CP Ti Grade 1 was much higher than that of AA1050, the centre and outer edges of CP Ti Grade 1 workpiece were subjected to insufficient thermal effect, leading to significant temperature difference and thermal concentration. The simulation results captured the combined effect of spindle speed and thermal conductivities on the temperature distribution.

Conclusions

This work presents an experimental and numerical investigation on the springback and surface finish of different materials in FSIF process, the main findings are outlined as follows:

(1) With an increase in spindle speed, the forming temperature increases and thus results in decrease of forming forces for both materials.

(2) Although under same processing condition, the surface finish and pattern of springback of the two materials are quite different due to the combined effect of spindle speed and thermal conductivities.
(3) Based on the results, it can be concluded that for material with high conductivity, the FSIF could be a viable option to achieve enhanced formability; whilst for sheet material with low conductivity, it would be better to use a different approach such as global heating (e.g., hot air heating) to obtain similar degree of formability improvement.

Acknowledgements
This work was supported by the UK Engineering and Physical Science Research Council [Grant No. EP/W010089/1].

References

[1] H. Zhu, H. Ou, A. Popov, Incremental sheet forming of thermoplastics: a review, The International Journal of Advanced Manufacturing Technology. 111 (2020) 565-587. https://doi.org/10.1007/s00170-020-06056-5

[2] W. Peng, H. Ou, Deformation mechanisms and fracture in tension under cyclic bending plus compression, single point and double-sided incremental sheet forming processes, International Journal of Machine Tools and Manufacture. 184 (2023) 103980. https://doi.org/10.1016/j.ijmachtools.2022.103980

[3] M. Li, R. Wu, S. Cai, Z. Chang, Z. Wang, J. Chen, Experimental investigation on friction-stir-assisted incremental forming with synchronous bonding of aluminum alloy and steel sheets, Journal of Materials Engineering and Performance. 29 (2020) 750-759. https://doi.org/10.1007/s11665-020-04600-8

[4] Z. Wang, S. Cai, J. Chen, Experimental investigations on friction stir assisted single point incremental forming of low-ductility aluminum alloy sheet for higher formability with reasonable surface quality, Journal of Materials Processing Technology. 277 (2020) 116488. https://doi.org/10.1016/j.jmatprotec.2019.116488

[5] P.A. Grün, E.H. Uheida, L. Lachmann, D. Dimitrov, G.A. Oosthuizen, Formability of titanium alloy sheets by friction stir incremental forming, The International Journal of Advanced Manufacturing Technology. 99 (2018) 1993-2003. https://doi.org/10.1007/s00170-018-2541-5

[6] A. Formisano, F. Lambiase, M. Durante, Polymer self-heating during incremental forming, Journal of Manufacturing Processes. 58 (2020) 1189-1199. https://doi.org/10.1016/j.jmapro.2020.09.031

[7] L. Li, J. Wang, Equivalent heating tool method for numerical simulation for sheet temperature in frictional stir incremental forming, The International Journal of Advanced Manufacturing Technology. 107 (2020) 1251-1263. https://doi.org/10.1007/s00170-020-05042-1

[8] S. Cai, R. Wu, Z. Wang, M. Li, J. Chen, Numerical simulation of friction stir-assisted incremental forming with synchronous bonding of heterogeneous sheet metals, The International Journal of Advanced Manufacturing Technology. 106 (2020) 2747-2763. https://doi.org/10.1007/s00170-019-04792-x

[9] N. Duc-Toan, P. Jin-Gee, K. Young-Suk, Combined kinematic/isotropic hardening behavior study for magnesium alloy sheets to predict ductile fracture of rotational incremental forming, International Journal of Material Forming. 3 (2010) 939-942. https://doi.org/10.1007/s12289-010-0923-9

[10] A. Giuseppina, C. Claudio, F. Luigino, G. Francesco, Theoretical model for temperature prediction in incremental sheet forming–experimental validation, International Journal of Mechanical Sciences. 108 (2016) 39-48. https://doi.org/10.1016/j.ijmecsci.2016.01.030

[11] G. Li, Z. He, J. Ma, H. Yang, H. Li, Springback analysis for warm bending of titanium tube based on coupled thermal-mechanical simulation, Materials. 14 (2021) 5044. https://doi.org/10.3390/ma14175044